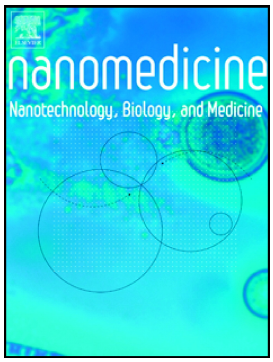

Epigallocatechin-3-gallate loaded PEGylated-PLGA nanoparticles: a new anti-seizure strategy for temporal lobe epilepsy

Amanda Cano, Miren Ettcheto, Marta Espina, Carmen Auladell, Ana Cristina Calpena, Jaume Folch, Marta Barenys, Elena Sánchez-López, Antoni Camins, Maria Luisa García

PII: S1549-9634(18)30031-5
DOI: doi:10.1016/j.nano.2018.01.019
Reference: NANO 1754

To appear in:

Received date: 26 July 2017
Revised date: 16 December 2017
Accepted date: 23 January 2018

Please cite this article as: Amanda Cano, Miren Ettcheto, Marta Espina, Carmen Auladell, Ana Cristina Calpena, Jaume Folch, Marta Barenys, Elena Sánchez-López, Antoni Camins, Maria Luisa García , Epigallocatechin-3-gallate loaded PEGylated-PLGA nanoparticles: a new anti-seizure strategy for temporal lobe epilepsy. The address for the corresponding author was captured as affiliation for all authors. Please check if appropriate. Nano(2018), doi:10.1016/j.nano.2018.01.019

Epigallocatechin-3-gallate loaded PEGylated-PLGA nanoparticles: a new anti-seizure strategy for temporal lobe epilepsy

Amanda Cano, MD[a,b], Miren Ettcheto, MD[c,d,e], Marta Espina, PhD[a,b], Carmen Auladell, PhD[f], Ana Cristina Calpena, PhD[a,b], Jaume Folch, PhD[e], Marta Barenys, PhD[c,g], Elena Sánchez-López, MD[a,b], , Antoni Camins, PhD[c,d,$] , Maria Luisa García, PhD[a,b,$*].

[a] Department of Pharmacy, Pharmaceutical Technology and Physical Chemistry, Faculty of Pharmacy and Food Sciences, University of Barcelona, Spain
[b] Institute of Nanoscience and Nanotechnology (IN2UB), Barcelona, Spain
[c] Department of Pharmacology, Toxicology and Therapeutic Chemistry, Faculty of Pharmacy and Food Sciences, University of Barcelona, Spain
[d] Biomedical Research Networking Centre in Neurodegenerative Diseases (CIBERNED), Madrid, Spain
[e] Unit of Biochemistry and Pharmacology, Faculty of Medicine and Health Sciences, University of Rovira i Virgili, Reus (Tarragona), Spain
[f] Department of Cellular Biology, Physiology and Immunology, Faculty of Biology, University of Barcelona, Spain.
[g] Institute of Nutrition Research and Food Safety (INSA-UB), University of Barcelona, Spain.

[$] Senior co-authors.

*__Corresponding author__: Maria Luisa García, Department of Pharmacy, Pharmaceutical Technology and Physical Chemistry, Faculty of Pharmacy and Food Sciences, University of Barcelona, Barcelona, Spain. E-mail address: marisagarcia@ub.edu / rdcm@ub.edu

Financial support

This work was supported by the Spanish Ministry of Science and Innovation (MAT 2014-59134-R and PI2016/01), CB06/05/0024 (CIBERNED) and the European Regional Development Founds. AC[a,b], ME[a,b], ACC[a,b], ESL[a,b] and MLG[a,b] belong to 2014SGR-1023. ME[c,d,e], CA[f], and AC[c,d] belong to 2014SGR-525. The first author, AC, acknowledges the support of the Generalitat de Catalunya for the PhD scholarship FI-DGR (CVE-DOGC-B-14206020-2014).

Conflict of interest

All authors do not have any actual or potential conflicts of interest including any financial, personal or other relationships with other people or organizations. All authors have reviewed the contents of the manuscript being submitted, approved its contents and validated the accuracy of the data.

Abstract

Temporal lobe epilepsy is the most common type of pharmacoresistant epilepsy in adults. Epigallocatechin-3-gallate has aroused much interest because of its multiple therapeutic effects, but its instability compromises the potential effectiveness. PEGylated-PLGA nanoparticles of Epigallocatechin-3-gallate were designed to protect the drug and to increase the brain delivery. Nanoparticles were prepared by the double emulsion method and cytotoxicity, behavioural, Fluoro-Jade C, Iba1 and GFAP immunohistochemistry studies were carried out to determine their effectiveness. Nanoparticles showed an average size of 169 nm, monodisperse population, negative surface charge, encapsulation efficiency of 95% and sustained release profile. Cytotoxicity assays exhibited that these nanocarriers were non-toxic. Behavioural test showed that nanoparticles reduced most than free drug the number of epileptic episodes and their intensity. Neurotoxicity and immunohistochemistry studies confirmed a decrease in neuronal death and neuroinflammation. In conclusion, Epigallocatechin-3-gallate PEGylated-PLGA nanoparticles could be a suitable strategy for the treatment of temporal lobe epilepsy.

Keywords: Epigallocatechin-3-gallate, polymeric nanoparticles, PLGA-PEG, epilepsy.

Abbreviations: AED, antiepileptic drugs; BBB, blood brain barrier; DSC, differential scanning calorimetry; EE, encapsulation efficiency; EGCG, epigallocatechin-3-gallate; FJ, Fluoro-Jade; FTIR, Fourier transform infrared spectroscopy; GFAP, glial fibrillary acidic protein; HPLC, high performance liquid chromatography; Iba1, ionized calcium-binding adapter 1; KA, kainic acid; NPs, nanoparticles; PEG, Polyethylene glycol; PI, polydispersity index; PLGA, poly(lactic-co-glycolic acid); SE, status epilepticus; TEM, transmission electron microscopy; TLE, temporal lobe epilepsy; WT, wild-type; Z_{av}, average particle size; ZP, zeta potential.

Background

Epilepsy is a disorder of the central nervous system derived from an imbalance in the electrical activity of neurons, which gives rise to convulsive events. The severity can range from mild attention deficit to intense convulsions, associated with a loss of consciousness. It is estimated that a third of patients do not respond to current treatments, increasing the prevalence of this disease 1% worldwide [1].

One of the most common forms of epilepsy in adulthood is the temporal lobe epilepsy (TLE). In most patients, TLE is considered medically intractable, with seizures often very physically and socially disabling. Besides, this type of epileptic disorder presents great differences among patients, having some of them a severe form resistant to antiepileptic drugs (AED) [2]. Recently, many studies are focused on finding new treatments for those forms of epilepsy, which do not respond to the available drugs[3,4].

Nowadays, one of the molecules that is mostly being evaluated for the treatment of many different diseases is the Epigallocatechin-3-gallate (EGCG). This polyphenol of the tea plant has the most potent biological activity [5]. A variety of studies have demonstrated that EGCG possess a beneficial pharmacological activity for chronic disorders such as cancer, down syndrome, diabetes or neurodegenerative diseases [5–7]. EGCG antioxidant activity is the main mechanism responsible for its beneficial health effects, but recent findings suggest many additional mechanisms of action such as modulation of metabolic enzymes or mitochondrial function [6,8,9].

Hippocampus is one of the most affected brain areas in the TLE, particularly susceptible to oxidative stress since it presents a low number of antioxidant systems [10–12]. Oxidative stress is related to neurochemical changes that occurs during seizures, due to the large detrimental alterations produced in the neuronal function during spontaneous recurrent seizures and status epilepticus (SE) [13]. A recent study of Kang et al. showed that EGCG decreased cell death processes and the neurotoxic effects produced by oxidative stress in the hippocampal area [14]. Noor et al. demonstrated that green tea extract treatment in rats ameliorated the state of oxidative stress during SE induced by pilocarpine [12]. Moreover Xie et al. showed that previous treatments with this drug ameliorated the oxidative damage and cognitive deficits

derived from pentylenetetrazole-induced seizures in rats [15]. Therefore, all these evidences suggest that EGCG could be an effective treatment for TLE.

Although this drug has a potential antiepileptic activity, the main problem of this type of molecules is its instability [16]. This fact significantly reduces the total amount of EGCG in a few hours, decreasing the bioavailability and effectiveness of the drug. For this reason there is an arising need to create a formulation that guarantees the stability and integrity of the EGCG [16–19].

In recent years, colloidal systems have been increasingly studied due to its potential for highly targeted drug delivery [20–22]. These systems act as a vector directing the drug to the site of action, improving its delivery and providing protection from external aggressions [20,23]. Smith et al. developed a nanolipidic system which improved both the penetration of EGCG through the blood brain barrier (BBB) as well as its oral bioavailability [24]. The main problem of these nanosystems is their short physical stability. In another study chitosan nanoparticles (NPs) of EGCG were designed, enhancing its intestinal absorption. However, the positive surface charge may increase the adherence to mucous membranes [25].

Among colloidal systems, one of the main alternatives are polymeric NPs. The major advantage of these systems are the sustained drug release and the reduction of the administered dose, which enables these particles to maintain therapeutic efficacy, decreasing adverse effects and improving patient adherence [26]. Furthermore, these particles are more stable than other nanosystems and can be easily lyophilized to prolong even more its integrity and the drug stability [27].

A variety of polymers have been selected to design NPs. One of the most widely used is poly (lactic-co-glycolic acid) (PLGA), approved by EMA (European Medicines Agency) and US FDA (Food and Drug Administration). The main reason is its safety, biocompatibility and biodegradability over time [28]. PEGylation of particles is one of the most common methods used to improve the properties of the NPs [29–31]. Polyethylene glycol (PEG), a non-ionic hydrophilic polyether, is extremely biocompatible and is commonly grafted onto the particle's surface to minimize immunogenicity and prolongs biological half-

life. Furthermore, conjugation of PEG to PLGA-based NPs reports others advantages which include enhanced aqueous solubility, suppressed opsonisation, reduced aggregation and improved NPs stability [32,33].

Therefore, the aim of this work is the development of EGCG PEGylated-PLGA NPs to protect the drug from the degradation and to evaluate the effectiveness of this new formulation for the treatment of TLE, using the chemically-induced model of kainic acid (KA) [34,35].

Methods

EGCG was purchased from Capotchem (Hangzhou, P.R.China) and diblock copolymer PLGA-PEG 5% Resomer® was obtained from Evonik Corporation (Birmingham, USA). Tween®80, β-glucuronidase (G-7396), sulfatase (S-9754) and KA (K-0250, monohydrate) were purchased from Sigma Aldrich (Madrid, Spain). The other reagents were of analytical grade.

Preparation of EGCG NPs

EGCG NPs were prepared by a modification of the W/O/W double emulsion-solvent evaporation technique described by Freytag et al. [36]. Tween®80 and ethyl acetate were the selected surfactant and oil phase, respectively. For details, see Supplementary Material.

Optimization study

In order to obtain the optimal formulation requiring a minimum of experiments, a 2^3 central composite factorial design was carried out [37]. The effect of the independent variables (EGCG, PLGA-PEG and Tween®80 concentrations) on the dependent variables (average particle size (Z_{av}), polydispersity index (PI), zeta potential (ZP) and encapsulation efficiency (EE)) was evaluated. Due to drug instability above pH 6 [16], a fixed pH value of 4.5 was defined. A total of 16 experiments were required according to the

design of the generated matrix, composed for 8 factorial points, 6 axial points and two replicated central points. The matrix central points were chosen according to pre-formulation assays (data not shown).

The responses were therefore modelled through the full second-order polynomial equation (Eq 1) (see description on Supplementary Material). Statgraphics Plus program, version 16.1.18 was the software used and the effect of the factors was evaluated by analysis of variance (ANOVA) [33].

$$Y = \beta_0 + \beta_1 X_1 + \beta_2 X_2 + \beta_3 X_3 + \beta_{11} X_1^2 + \beta_{22} X_2^2 + \beta_{33} X_3^2 + \beta_{12} X_1 X_2 + \beta_{13} X_1 X_3 + \beta_{23} X_2 X_3 \quad /1/$$

Physicochemical and morphological characterization

To determinate the Z_{av} and PI, a morphometric analysis through photon correlation spectroscopy was carried out in a Zetasizer Nano ZS (Malvern Instruments, Malvern, UK). Samples were diluted (1:10) and were read at 25°C by triplicate. ZP, which is related with the rate of aggregation of particles, was evaluated by using laser-doppler electrophoresis with M3 PALS system in Zetasizer Nano ZS. A greater ZP (in absolute value) would indicate less aggregation due to repulsion forces between the NPs. Henry equation (see description on Supplementary Material) was used to calculate this parameter (Eq 2):

$$\mu_E = \frac{\varepsilon Z P f(Ka)}{6\pi\eta} \quad /2/$$

Transmission electron microscopy (TEM) was used to investigate the morphology of the EGCG NPs on a Jeol 1010 (CA, USA). Copper grids were activated with UV light and samples were diluted (1:10) and placed on the grid surface to visualize the particles. Samples were previously subjected to negative staining with uranyl acetate (2%).

Determination of the encapsulation efficiency

EE was determined indirectly by measuring the amount of free drug in the formulation dispersion medium (Eq 3). Free EGCG was separated from NPs by filtration/centrifugation using an Amicon® Ultra-0.5 centrifugal filter devices (Millipore® Co, Massachusetts, USA).

$$\mathrm{EE}(\%) = \frac{\text{Total amount of EGCG} - \text{Free amount of EGCG}}{\text{Total amount of EGCG}} \cdot 100$$

/3/

The amount of EGCG was evaluated by high performance liquid chromatography (HPLC), as described by Fangueiro et al. 2014 [38]. Standards with a concentration range from of 0.01 to 0.20 mg/ml were prepared. Data was processed using Empower 3®Software.

Interaction studies

Differential scanning calorimetry (DSC) analysis was performed using a Mettler Toledo DSC 823e System (Mettler Toledo, Spain). Approximately 2-3 mg of different components of the formulation were filled into 40 µl aluminium pans and sealed. Mettler TA 4000 system (Greifensee, Switzerland) equipped with a DSC 25 cell was used to obtain thermograms, which were analyzed using the Mettler STARe V 9.01 DB software. Maximum peaks of the heating curves correspond to melting points of the compounds.

Fourier transform infrared (FTIR) spectra of different components of NPs were obtained using a Thermo Scientific Nicolet iZ10 with an ATR diamond and DTGS detector (Wisconsin, USA).

In both studies NPs were centrifuged (Optima® LE-BOK Ultracentrifuge, Beckman, USA) using a polycarbonate centrifuge bottle (Beckman Coulter, Inc. Brea, USA) at 15ºC and 15000 rpm for 15 minutes. The obtained pellet was collected, dried and pulverized for the analysis of the samples.

Determination of in vitro release profile

Due to the high water solubility of EGCG, *in vitro* release profile was evaluated using direct dialysis bag technique [39]. Two different release mediums were chosen: the first one was composed of an acid buffer solution (pH 4.5) with ascorbic acid 0.25%; the second one was PBS 0.1M buffer solution (pH 7.4). The dialysis sacs were equilibrated with the dissolution medium 1 hour before the start of the experiment. NPs and free EGCG samples (5 ml) enclosed in dialysis bags (Medicell International Ltd. MWCO 12-14000,

London, UK) were placed in 70 ml of buffers at 37 °C under magnetic stirring. The assay was carried out by triplicate. At predetermined time intervals, 1 ml of samples were withdrawn from the release medium to be analyzed with HPLC using the conditions described above, and replaced with buffer solution. Different kinetic models were used to adjust the data [40].

Short term stability of NPs

The assessment of the stability of NPs was performed using the optical analyzer Turbiscan®Lab (Formulation, L'Union, France), as described Vega et al. [29]. Samples were scanned every hour, during a period of 24 hours. Backscattering measure was monthly performed for 6 months, as well as Z_{av}, PI and ZP.

Cytotoxicity assays

To know the cellular viability of the target organ the dye Alamar Blue indicator was used [41]. Absorbance was determined at λ of 570 nm (reduced form) and 620 nm (oxidized form) after incubating the cells (astrocytes, bEnd.3 and PC12 cells) with the samples at different concentrations for 24 hours. Data were analysed by calculating the percentage of Alamar blue reduction and expressed as percentage of control.

Animals

1-month old wild-type (WT) C57BL/6J mice were purchased from Harlan Laboratories, Inc (IN, USA). Animals had ad lib access to food and water under a 12:12 hours light:dark cycle. Animal procedures were conducted according to ethical guidelines (European Communities Council Directive 2010/63/EU), the procedures established by the Department d'Agricultura, Ramaderia i Pesca of the Generalitat de Catalunya, and approved by the local ethical committee (University of Barcelona). Many efforts were made to reduce the number of animals as much as possible maintaining the significance of the results, and to minimize the suffering of animals.

Hemolysis in vitro test

Since polymers are most commonly used in biomedical applications, it is necessary to assess the biocompatibility of the NPs. The hemolytic activity of the NPs was tested as described elsewhere with some modifications [42]. Mice blood was used to evaluate both samples. Distilled water and NaCl 0.9% were used as positive and negative control, respectively. The absorbance of oxidized haemoglobin (OxHb) was used as hemolysis indicator, and its absorbance was measured at 540 nm. For more details, see Supplementary material.

Pharmacokinetic assay

An in vivo pharmacokinetic assay was performed as described Cheng et al[43]. Briefly, 30 mg/kg of free drug and EGCG NPs were injected to mice intraperitoneally (i.p.) and sacrificed at different times. Blood samples were drawn by cardiac puncture to analyze drug levels in plasma, and brain was removed at the end of the experiment to evaluate the drug amount.

Plasma was extracted by centrifugation of blood samples with a 20% ascorbic acid 0.5 mg/ml Na_2EDTA PBS 0.4M solution, and tissue sample by homogenization/centrifugation in the same solution. Samples were then incubated with 10 μL of β-glucuronidase (250U) and sulfatase (1U) for 45 minutes at 37 °C, extracted with ethyl acetate twice and resuspended in an acetonitrile 10% ascorbic acid 20% solution to detect the drug amount on HPLC-MS-MS [44]. Plasma/brain samples were run by triplicate.

Behavioural assessment of seizure threshold

One of the most common substances for chemically-induced TLE is KA. Systemic administration of KA has been widely used as a model for TLE since it reproduces many features of the disorder [35]. Mice were divided in WT group (n=10), WT+KA group (n=10), WT+KA+free EGCG group (n=16) and WT+KA+EGCG NPs group (n=16). To study the effectiveness of the drug against seizures and their neural effects the formulations were evaluated as described Morrison et al. with some modifications [45]. Briefly, EGCG NPs and free EGCG were administered by i.p. at a 30 mg/kg body weight dose 2 and 1 hours respectively before KA injection to 8 to 10-week old mice. KA was also administered i.p. at a 25 mg/kg body weight dose. Animals were observed during 2 hours after KA injection to evaluate the

severity and duration of seizure activity (Table S1 of Supplementary material). The different seizure behaviours were scored on a scale from 0 (normal behaviour) to 7 (death). For more details, see Supplementary Material.

Tissue preparation

Animals were sacrificed 24 and 72 hours after KA injection. All mice were anesthetized by i.p. injection of sodium pentobarbital (80 mg/kg) and perfused with paraformaldehyde 4% in phosphate buffer 0.1 M. Brains were removed and subsequently rinsed in paraformaldehyde 4% with 30% sacarose for 24 h and then frozen at -80^{o}C. Coronal sections of 20 μm were obtained by a cryostat (Leica Microsystems, Wetzlar, Germany).

Fluoro-Jade C staining

Brains from mice sacrificed after 24 hours of KA injection were used for Fluoro-Jade C (FJ) staining to evaluate neurodegeneration as described elsewhere[46]. Briefly, slides were immersed in 0.06 g/l of $KMnO_4$ and transferred to the staining solution containing 0.1 % of acetic acid and 0.0001% of Fluoro-Jade C for 30 minutes in the dark. Then, the slides were dried, submerged in xylene and mounted in DPX medium. They were analysed with an epifluorescence microscope (Olympus BX61, Barcelona, Spain).

Immunohistochemistry studies

Ionized calcium-binding adapter 1 (Iba1) and glial fibrillary acidic protein (GFAP) expression together were selected as indicators of neuroinflammation. Brains from mice sacrificed after 24 h and 3 days of KA injection were used for Iba1 and GFAP immunohistochemistry respectively. These studies were carried out as previously described Ettcheto et al [47]. Primary polyclonal antibodies against Iba1 (1:1000, Wako Chemicals, Richmond, VA, USA) and GFAP (1:1000; Dako Chemicals, Glostrup, Denmark) were used. Iba1 and GFAP positive cells were also counted blinded under fluorescent field using 10x magnification in all the samples. For detailed description, see Supplementary material.

Statistical analysis

Data are presented as the mean ± S.D. One-way ANOVA followed by Tukey post hoc test was performed for groups comparison. Statistical significance was set at $p<0.05$ by using GraphPad 6.00 Prism.

Results

Optimization study

Table 1 shows the results obtained in the optimization study. Regarding to Z_{av}, the most influential variables were the percentage of Tween®80 and the amount of polymer, being inversely proportional to the concentration of surfactant, and directly proportional to the concentration of polymer (Figure 1A). The analysis of PI showed that the most influential parameters were the EGCG and Tween®80 concentrations (Figure 1B). ZP was greatly influenced by the concentration of surfactant, increasing in absolute value as this variable increase (Figure 1C). Higher concentrations of EGCG did not significantly affect EE, suggesting that the developed NPs could be loaded with larger amounts of drug than those studied in this factorial design.

To promote drug release from the polymeric matrix, the highest drug loading formulation and the lowest amount of surfactant able to maintain good characteristics were selected.

Physicochemical and morphological characteristics

The trend of the results was analysed and a final formulation with 1.5 mg/ml of EGCG, 14 mg/ml of PLGA-PEG and Tween®80 1.5% was selected. These characteristics led to a monodisperse population (PI < 0.1) of particles with a Z_{av} of 168.5 ± 9.9 nm and a EE higher than 95%. This particle size (lower than 200 nm) and the surfactant selected (Tween®80) improve the penetration of NPs through the BBB [48–50]. Although the PEG layer reduces the surface negative charge of PLGA-NPs [51], the optimized formulation showed a ZP value (-23.3 ± 5.3 mV) large enough to increase the repulsion forces between the NPs, thereby increasing the stability of the sample. As is shown in Figure 1D, PEG chains were oriented

towards the aqueous phase creating a hydrophilic layer surrounding the particles. Furthermore, TEM images (Figure 1D) revealed that the particles had a smooth surface and spherical shape without signals of aggregation phenomena.

Interaction studies

DSC analysis was used to determine the physical state of EGCG and the components of NPs formulation (Figure 2A). DSC thermogram of EGCG showed an endothermic peak at 225^{o}C which corresponds to its melting transition, follows by an exothermic peak at 235^{o}C which coincides to a process of melting decomposition of the drug. Interestingly, these peaks were not observed in EGCG NPs profile suggesting that the entire drug amount was completely loaded inside the polymeric matrix. The conversion of the crystalline form of drug into a disordered crystalline, amorphous or solid solution state inside the NPs explains this fact [52]. A slight variation between the initiation of the glass transition (T_g) of the polymer and NPs was observed, due to the drug-polymer interaction. This phenomenon could be due to the effect of the drug on the weak interactions of PLGA [51,53].

To evaluate the interactions between the drug and PLGA-PEG, the FTIR technique was used (Figure 2B). No evidence of covalent bonds between EGCG and any component of NPs was observed. Drug-loaded and empty NPs showed very similar pattern between them, and also similar to the polymer bands. The loaded NPs evidenced a decrease in absorbance due to the drug content. EGCG FTIR profile shows a characteristic peak at 3356 cm^{-1} for the OH group attached to the aromatic ring. Also appeared others bands at 1077, 1199 and 1305 cm^{-1} in the NPs and polymer spectrum which correspond to stretching vibrations of the OH group. In the 1500 to 1700 cm^{-1} arrange a series of peaks appear, of which 1690 cm^{-1} peak corresponds to C=O group that links the chroman and trihydroxybenzoate groups, and 1543 cm^{-1} peak corresponds to C-C stretch in aromatic ring [52,54].

In vitro release profile

The *in vitro* cumulative drug release profile revealed a sequential and controlled release of EGCG. Drug release in acid buffer solution and PBS was around 40% and 30% respectively of the total entrapped drug for 7 days (Figure 3A). These results are in agreement to those obtained by other authors for drug-loaded PLGA-casein core shell NPs [42]. EGCG showed an initial burst (21.1 ± 2.1% in acid buffer and 17.0 ± 2.9% in PBS) owing to the superficially entrapped drug. This fact was followed by a slowly process of drug sustained release from polymer matrix to the dialysis medium. Controlled release systems of PLGA matrices usually show an initial burst with a zero-order release profile [55], and drugs can be released from the polymeric matrix by different routes, either by erosion of the polymer, diffusion through the PLGA-PEG matrix, or a mixture of both [29,51]. Free EGCG showed faster release kinetics than EGCG-loaded NPs. After 6 hours, the free drug achieved >90% release, whereas the NPs released were around 10% of the initial amount. The best fit with the highest correlation was found for the hyperbola model for free EGCG (r^2=0.9896), EGCG NPs in acid buffer (r^2=0.9779) and EGCG NPs in PBS (r^2=0.9722), indicating a diffusion-governed release.

Stability of NPs

As shown in Figure 3B no backscattering alteration was observed for NPs stored at 4°C, which means that NPs maintained their morphometric characteristics during this period. Instead, NPs stored at 25°C showed a decrease of the backscattering profile at the sixth month of the study (Figure 3C). There was also a significant decrease of the surface charge (-23.1±0.5 to -14.8±0.7 mV) and Z_{av} (176.6±1.2 to 76.8±9.2 nm) in agreement with backscattering results (Table S2 of supplementary material). Both facts may be due to degradation of the polymer matrix [55]. A brown coloration was also observed in the NPs stored at 25°C, but not at 4°C (Figure S1 of supplementary material). This fact may be due to the release of the drug into the medium and its consecutive oxidation, confirming the importance of temperature in the stabilization process of NPs and the drug.

Hemolysis in vitro test and cytotoxicity assays

The results of the hemolytic test demonstrated that the hemolysis rates of the samples were lower than 5% (Figure 4A). These results indicate that EGCG NPs and free drug showed a non-hemolytic effect up to 1.5

mg/ml. Results of cytotoxicity assay are shown in Figure 4B. For lower concentrations than 1.25%, cell viability was higher than 80% in all lines, thus meaning that EGCG NPs do not damage neither endothelial brain cells nor neuronal cells at these concentrations.

Pharmacokinetic assay

Results obtained in pharmacokinetic assay showed that free drug exhibited a faster absorption than encapsulated drug, with a T_{max} value 20 minutes lower than EGCG-loaded NPs. However, EGCG administered in NPs maintained plasma levels up to 240 minutes after its administration whereas free drug was undetectable after 90 minutes (Figure 5). It can be explained by the increase of EGCG permanence in blood, caused by the polymer matrix itself and the incorporation of PEG to the nanosystem [56]. Pharmacokinetic parameters are showed in Table 3. EGCG brain amount was measured at 8 hours. Free EGCG and EGCG NPs showed a concentration of 4.874±0.928 and 4.075±1.052 ng/mg respectively.

Behavioural assessment of seizure threshold

Behavioural assessment results are described in Table 2. As shown in Figure 6, pre-emptive injection of free EGCG previous to the KA administration reduced significantly ($p<0.0001$) the TLE convulsive pattern on the animals. Mice treated with the free drug showed a 36.6 % lower score than WT+KA group. In addition, WT+KA+EGCG NPs group showed more significant results than the free drug ($p<0.05$), obtaining a test score 56.1 % lower than WT+KA group ($p<0.0001$).

Reduction of neurodegeneration in EGCG NPs pre-treated mice

FJ^+ neurons were only detected in WT+KA group, being the amygdala, cortex, hypothalamus and paraventricular and intermediodorsal nucleus of the thalamus the most affected areas (Figure 7). No FJ^+ neurons were observed in any brain area of WT and pre-treated groups (Figure S2 of Supplementary material). These results corroborate that both free EGCG and EGCG NPs pre-treatment protects from neuronal toxicity.

Reduction of glial reactivity in EGCG NPs pre-treated mice

Iba1 and GFAP immunoreactivity of pre-treated groups revealed a thin labelling typical of healthy individuals, while WT+KA group showed heavily activated cells which were present especially in the hippocampus region (Figure 8A and 8B). Counting rates of reactive cells revealed a significant decrease in the number of Iba1 and GFAP positive cells in different brain regions of WT and pre-treated groups compared with WT+KA group (Figure 8C). Non-significant differences were obtained between EGCG NPs and free EGCG administration in Iba1 immunohistochemical results. In contrast, there was observed a significant decrease in the number of GFAP positive cells in the WT+KA+EGCG NPs group compared with the free drug, which may be caused by the prolonged release of the drug from the polymeric matrix.

Discussion

The major finding of the current study is the significant decrease in the number and intensity of the seizure pattern together with a diminution of neuropathological alterations in a mouse model of TLE by the EGCG PEGylated-PLGA NPs pre-treatment. The results evidenced that EGCG possesses an effective anticonvulsant activity which is ameliorated by the developed nanostructured system.

TLE is the most common type of drug-resistant epilepsy. Patients with TLE typically have complex seizures with secondary generalization. Many reasons, such as the appearance of the SE itself, cause a failed response to a sequential treatment with first- and second-line AEDs [57]. In the last years, many efforts have been made to find new drugs for this type of epilepsy. In the current paper we attempted to demonstrate the effectiveness of EGCG as a new therapeutic alternative for TLE. Although being it is a promising drug, EGCG is rapidly degraded because of its chemical nature. Thus, one of the alternatives to improve the stability of drugs increasing their bioavailability are the controlled drug delivery systems.

In the present study EGCG-loaded PLGA-PEG NPs were successfully synthesized. Narayanan et al. developed a PLGA-casein core shell NPs of EGCG and Paclitaxel, with a particle size of 230.0 ± 27.0 nm which increased upon precipitation of casein containing EGCG onto the PLGA core. Moreover, PI was near to a bimodal population [42]. Both characteristics may compromise the penetration of the NPs into the

brain. In our study EGCG NPs presented a uniform size distribution around 170 nm and monodisperse population, spherical morphology, excellent physical stability supported by high negative surface charge, and a drug loading capacity higher than 95%. Moreover, the developed polymeric nanosystem showed a stability of at least 6 months at low storage temperatures, thereby prolonging the integrity of the drug. The *in vitro* release study exhibited a prolong release of EGCG from the polymeric matrix, contributing towards a decrease of the drug regime dosage and therefore improving the patient adherence to the treatment. On the other hand, interaction studies also demonstrated that the EGCG was integrated into the NPs and there were no covalent bonds between drug and polymer. This phenomenon contributes to a suitable release of the drug from the polymer matrix. All these features provide the developed nanosystem the capacity to protect the EGCG and facilitate its penetration into the central nervous system.

Cytotoxicity studies and hemolysis test showed both that the optimized formulation did not affect cell viability neither on bEnd.3, astrocytes, PC12 nor red blood cells. These results confirm that EGCG NPs are biocompatible and non-toxic to the organism, and can be administered by different routes.

EGCG-loaded NPs showed a prolonged permanence time in blood than free drug, which can be explain by the protection of the drug from the renal clearance due to the increased size and liver enzyme metabolism[56]. Furthermore, polymeric surface modification with PEG minimize the opsonisation, reducing the reticuloendothelial system uptake and increasing circulation half-life[56].

KA-induced epilepsy mouse model was chosen to carry out a behavioural assessment [58]. Our results showed that EGCG NPs were significantly ($p<0.05$) more effective than free EGCG, decreasing the duration and severity of seizure activity. These positive results can be attributed to encapsulation and drug protection into PLGA-PEG NPs since PEGylation contributes to increase the penetration across the BBB [16,19,59].

The neuropathological analyses evidenced the neuroprotective effect of EGCG since a reduction of FJ+ neurons and a decrease in the glial response were observed with both free EGCG and EGCG NPs pre-treatment before KA injection. Both microglia and astrocytes act as a support for a wide variety of inflammatory mediators during seizures, which are proposed to contribute to neurodegeneration[60]. Ex vivo fluorescence images of the brains showed an enlarged cell body and drastically changes in astrocyte

morphology in WT+KA group, not instead in pre-treated animals. No significant differences were found in the results obtained in neurotoxicity and neuroinflammation studies at 24 hours after exposure to KA between formulations, both were equally effective. This is in agreement with the results obtained in the pharmacokinetic assay, since the EGCG brain amount at first hours after drug administration were similar when it was administered as free drug and encapsulated in NPs. However, a significant decrease in the GFAP counting rate was observed in EGCG NPs group compared with the free EGCG group. Due to GFAP study was carried out in mice which were sacrificed 3 days after KA injection, this result suggests that prolonged release of EGCG from NPs is a clear advantage to protect from the damage caused during the SE in the long term. All these results are also in accordance with behavioural assay.

In conclusion, the current study demonstrates that EGCG PEGylated-PLGA NPs significantly improve the anticonvulsive and neuroprotective effect of the free drug, mainly reducing the neuroinflammatory process and seizure threshold. In addition, EGCG NPs are safe for the brain cells and capable of increasing drug integrity and bioavailability. For these reasons we suggest that EGCG-loaded PEGylated PLGA NPs could be a promising, effective and safe strategy for the treatment and prevention of TLE.

References

1. Cunliffe, V. T. Building a zebrafish toolkit for investigating the pathobiology of epilepsy and identifying new treatments for epileptic seizures. *Journal of Neuroscience Methods* **260,** 91–95 (2016).

2. AlQassmi, A., Burneo, J. G., McLachlan, R. S. & Mirsattari, S. M. Benign mesial temporal lobe epilepsy: A clinical cohort and literature review. *Epilepsy & Behavior* **65,** 60–64 (2016).

3. Burtscher, J. & Schwarzer, C. The Opioid System in Temporal Lobe Epilepsy : Functional Role and Therapeutic Potential. *Frontiers in Molecular Neuroscience* **10,** 1–13 (2017).

4. Mirza, N., Sills, G. J., Pirmohamed, M. & Marson, A. G. Identifying new antiepileptic drugs through genomics- based drug repurposing. *Human Molecular Genetics* **26,** 527–537 (2017).

5. Chowdhury, A., Sarkar, J., Chakraborti, T., Pramanik, P. K. & Chakraborti, S. Protective role of epigallocatechin-3-gallate in health and disease: A perspective. *Biomedicine and Pharmacotherapy* **78,** 50–59 (2016).

6. Kim, H. S., Quon, M. J. & Kim, J. a. New insights into the mechanisms of polyphenols beyond antioxidant properties; lessons from the green tea polyphenol, epigallocatechin 3-gallate. *Redox Biology* **2,** 187–195 (2014).

7. de la Torre, R., Sola, S., Hernández, G., Farré, M., Pujol, J., Rodríguez, J. *et al.* Safety and efficacy of cognitive training plus epigallocatechin-3-gallate in young adults with Down's syndrome (TESDAD): A double-blind, randomised, placebo-controlled, phase 2 trial. *The Lancet Neurology* **15,** 801–810 (2016).

8. Singh, B. N., Shankar, S. & Srivastava, R. K. Green tea catechin, epigallocatechin-3-gallate (EGCG): Mechanisms, perspectives and clinical applications. *Biochemical Pharmacology* **82,** 1807–1821 (2011).

9. Oliveira, M. R. De, Nabavi, S. F., Daglia, M., Rastrelli, L. & Nabavi, S. M. Epigallocatechin gallate and mitochondria - A story of life and death. *Pharmacological Research* **104,** 70–85

(2016).

10. de Freitas, R. . Lipoic Acid Alters δ-Aminolevulinic Dehydratase, Glutathione Peroxidase and Na+,K+-ATPase Activities and Glutathione-Reduced Levels in Rat Hippocampus After Pilocarpine-Induced Seizures. *Cell Mol Neurobiol* **30,** 381–387 (2010).

11. Pires, L. F., Muratori, L., Cardoso de Almeida, A.A.,Almeida, O., Santos, G., Pergentino, D. *et al.* Neuropharmacological effects of carvacryl acetate on δ-aminolevulinic dehydratase, Na+, K+-ATPase activities and amino acids levels in mice hippocampus after seizures. *Chemico-biological interactions* **226,** 49–57 (2015).

12. Noor, N. A., Mohammed, H. S., Khadrawy, Y. a., Aboul Ezz, H. S. & Radwan, N. M. Evaluation of the neuroprotective effect of taurine and green tea extract against oxidative stress induced by pilocarpine during status epilepticus. *The Journal of Basic & Applied Zoology* **72,** 8–15 (2015).

13. Barros, D. O., Xavier, S.M.L., Barbosa, C.O., Silva, R.F., Freitas, R.L.M., Maia, F.D. *et al.* Effects of the vitamin E in catalase activities in hippocampus after status epilepticus induced by pilocarpine in Wistar rats. *Neuroscience Letters* **416,** 227–230 (2007).

14. Kang, K. S, Wen, Y., Yamabe, N., Fukui, M., Bishop, S.C., Zhu, B.T. *et al.* Dual beneficial effects of (-)-epigallocatechin-3-gallate on levodopa methylation and hippocampal neurodegeneration: In vitro and in vivo studies. *PLoS ONE* **5,** 1–12 (2010).

15. Xie, T., Wang. W.P., Mao, Z.F., Qu, Z.Z., Luan, S.Q., Jia, L.J. & Kan MC. . Neuroscience Letters Effects of epigallocatechin-3-gallate on pentylenetetrazole-induced kindling , cognitive impairment and oxidative stress in rats. *Neuroscience Letters* **516,** 237–241 (2012).

16. Krupkova, O., Ferguson, S. J. & Wuertz-Kozak, K. Stability of (-)-epigallocatechin gallate and its activity in liquid formulations and delivery systems. *Journal of Nutritional Biochemistry* **37,** 1–12 (2016).

17. Fangueiro, J. F., Calpena., A.C., Clares, B., Andreani, T., Egea, M.A., Veiga, F.J. *et al.* Biopharmaceutical evaluation of epigallocatechin gallate-loaded cationic lipid nanoparticles

(EGCG-LNs): In vivo, in vitro and ex vivo studies. *International Journal of Pharmaceutics* **502,** 161–169 (2016).

18. Fangueiro, J. F, Andreani, T., Fernandes, L., García, M.L., Egea, M.A., Silva, A.M. *et al.* Physicochemical characterization of epigallocatechin gallate lipid nanoparticles (EGCG-LNs) for ocular instillation. *Colloids and Surfaces B: Biointerfaces* **123,** 452–460 (2014).

19. Dube, A., Ng, K., Nicolazzo, J. A. & Larson, I. Effective use of reducing agents and nanoparticle encapsulation in stabilizing catechins in alkaline solution. *Food Chemistry* **122,** 662–667 (2010).

20. Tam, V. H., Sosa, C., Liu, R., Yao, N. & Priestley, R. D. Nanomedicine as a non-invasive strategy for drug delivery across the blood brain barrier. *International Journal of Pharmaceutics* **515,** 331–342 (2016).

21. Yokel, R. A. Physicochemical properties of engineered nanomaterials that influence their nervous system distribution and effects. *Nanomedicine: Nanotechnology, Biology, and Medicine* **12,** 2081–2093 (2016).

22. Parveen, S., Misra, R. & Sahoo, S. K. Nanoparticles : a boon to drug delivery , therapeutics , diagnostics and imaging. *Nanomedicine: Nanotechnology, Biology, and Medicine* **8,** 147–166 (2012).

23. Ramezanli, T., Zhang, Z. & Michniak-kohn, B. B. Development and characterization of polymeric nanoparticle-based formulation of adapalene for topical acne therapy. *Nanomedicine: Nanotechnology, Biology, and Medicine* **13,** 143–152 (2017).

24. Smith, A., Giunta. B., Bickford, P.C., Fountain, M., Tan, J. & Shytle R.D. Nanolipidic particles improve the bioavailability and α-secretase inducing ability of epigallocatechin-3-gallate (EGCG) for the treatment of Alzheimer ' s disease. *International Journal of Pharmaceutics* **389,** 207–212 (2010).

25. Dube, A., Nicolazzo, J. A. & Larson, I. Chitosan nanoparticles enhance the plasma exposure of (-)-epigallocatechin gallate in mice through an enhancement in intestinal stability. *European*

Journal of Pharmaceutical Sciences **44,** 422–426 (2011).

26. Patel, T., Zhou, J., Piepmeier, J. M. & Saltzman, W. M. Polymeric nanoparticles for drug delivery to the central nervous system. *Advanced Drug Delivery Reviews* **64,** 701–705 (2012).

27. Rosario, G., Calpena, A.C., Egea, M.A., Espina, M. & García, M.L. Freeze drying optimization of polymeric nanoparticles for ocular flurbiprofen delivery : effect of protectant agents and critical process parameters on long-term stability. **9045,** (2017).

28. Sharma, S., Parmar, A., Kori, S. & Sandhir, R. PLGA-based nanoparticles: a new paradigm in biomedical applications. *TrAC Trends in Analytical Chemistry* **80,** 30–40 (2015).

29. Vega, E., Egea M.A., Garduño-Ramírez, M.L., García, M.L., Sánchez, E., Espina, M. *et al.* Flurbiprofen PLGA-PEG nanospheres: Role of hydroxy-β-cyclodextrin on ex vivo human skin permeation and in vivo topical anti-inflammatory efficacy. *Colloids and Surfaces B: Biointerfaces* **110,** 339–346 (2013).

30. Kolate, A., Baradia, D., Patil, S., Vhora, I., Kore, G. & Misra, A. PEG - A versatile conjugating ligand for drugs and drug delivery systems. *Journal of Controlled Release* **192,** 67–81 (2014).

31. Huang, N., Cheng, S., Zhang, X., Tian, Q. & Pi, J. Efficacy of NGR peptide-modified PEGylated quantum dots for crossing the blood – brain barrier and targeted fluorescence imaging of glioma and tumor vasculature. *Nanomedicine: Nanotechnology, Biology, and Medicine* **13,** 83–93 (2017).

32. El-Hammadi, M. M., Delgado, Á. V., Melguizo, C., Prados, J. C. & Arias, J. L. Folic acid-decorated and PEGylated PLGA nanoparticles for improving the antitumour activity of 5-fluorouracil. *International Journal of Pharmaceutics* **516,** 61–70 (2017).

33. Sánchez-lópez, E., Ettecheto, M., Egea, M.A, Espina, M., Calpena, A.C., Folch, J. *et al.* New potential strategies for Alzheimer' s disease prevention : pegylated biodegradable dexibuprofen nanospheres administration to APPswe / PS1dE9. *Nanomedicine: Nanotechnology, Biology, and Medicine* **13,** 1171–1182 (2017).

34. Levesque, M., Avoli, M. & Bernard, C. Animal models of temporal lobe epilepsy following

systemic chemoconvulsant administration. *Journal of Neuroscience Methods* **260,** 45–52 (2016).

35. Jefferys, J., Steinhäuser, C. & Bedner, P. Chemically-induced TLE models: Topical application. *Journal of Neuroscience Methods* **260,** 53–61 (2016).

36. Freytag, T., Dashevsky, A., Tillman, L., Hardee, G. E. & Bodmeier, R. Improvement of the encapsulation efficiency of oligonucleotide-containing biodegradable microspheres. *Journal of Controlled Release* **69,** 197–207 (2000).

37. Gonzalez-Mira, E., Egea, M. A., Garcia, M. L. & Souto, E. B. Design and ocular tolerance of flurbiprofen loaded ultrasound-engineered NLC. *Colloids and Surfaces B: Biointerfaces* **81,** 412–421 (2010).

38. Fangueiro, J. F., Parra, A., Silva, A.M., Egea, M.A., Souto, E.B., García, M.L. *et al.* Validation of a high performance liquid chromatography method for the stabilization of epigallocatechin gallate. *International Journal of Pharmaceutics* **475,** 181–190 (2014).

39. Puri, S., Kallinteri, P., Higgins, S., Hutcheon, G. A. & Garnett, M. C. Drug incorporation and release of water soluble drugs from novel functionalised poly(glycerol adipate) nanoparticles. *Journal of Controlled Release* **125,** 59–67 (2008).

40. Gonzalez-Mira E, Nikolic S, Calpena AC, Egea MA, Souto EB, G. M. Improved and safe transcorneal delivery of flurbiprofen by NLC and NLC-based hydrogels. *J. Pharm. Sci.* **101,** 707–25 (2012).

41. Bonnier, F. *et al.* Toxicology in Vitro Cell viability assessment using the Alamar blue assay : A comparison of 2D and 3D cell culture models. *Toxicology in vitro* **29,** 124–131 (2015).

42. Narayanan, S., Pavithran, M., Viswanath, A., Narayanan, D., Mohan, C.C., Manzoor, K. *et al.* Sequentially releasing dual-drug-loaded PLGA-casein core/shell nanomedicine: Design, synthesis, biocompatibility and pharmacokinetics. *Acta Biomaterialia* **10,** 2112–2124 (2014).

43. Chen, L., Lee, M., Li, H. E., Yang, C. S. & Al, C. E. T. Absorption , distribution , and elimination of tea polyphenols in rats abstract. *Drug Metab. Dispos.* **25,** 0–5 (1997).

44. Mata-Bilbao, M.L., Roura, E., Jáuregui, O., Torre, C., & Lamuela-Raventós, R.M. New LC / MS / MS Rapid and Sensitive Method for the Determination of Green Tea Catechins and their Metabolites in Biological Samples. *J. Agric. Food Chem* **55,** 8857–8863 (2007).

45. Morrison, R. S., Wenzel, H.J., Kinoshita, Y., Robbins, C.A., Donehower, L.A. & Schwartzkroin, P.A. Loss of the p53 tumor suppressor gene protects neurons from kainate-induced cell death. *Journal of Neuroscience* **16,** 1337–1345 (1996).

46. Gu, Q., Schmued, L. C., Sarkar, S., Paule, M. G. & Raymick, B. One-step labeling of degenerative neurons in unfixed brain tissue samples using Fluoro-Jade C. *Journal of Neuroscience Methods* **208,** 40–43 (2012).

47. Ettcheto, M., Petrov, D., Pedrós, I., Alva, N., Carbonell, T., Beas-Zarate, C. *et al.* Evaluation of Neuropathological Effects of a High-Fat Diet in a Presymptomatic Alzheimer ' s Disease Stage in APP / PS1 Mice. *Journal of Alzheimer's Disease* **54,** 233–251 (2016).

48. Calvo, P., Gouritin, B., Brigger, I., Lasmezas, C., Deslus, J., Williams, A. *et al.* PEGylated polycyanoacrylate nanoparticles as vector for drug delivery in prion diseases. *Journal of Neuroscience Methods* **111,** 151–155 (2001).

49. Soppimath, K. S., Aminabhavi, T. M., Kulkarni, A. R. & Rudzinski, W. E. Biodegradable polymeric nanoparticles as drug delivery devices. *Journal of Controlled Release* **70,** 1–20 (2001).

50. Kreuter, J. Drug delivery to the central nervous system by polymeric nanoparticles: What do we know? *Advanced Drug Delivery Reviews* **71,** 2–14 (2014).

51. Sánchez-López, E., Egea, M.A., Cano, A., Espina, M., Calpena, A.C., Ettecho, M. *et al.* PEGylated PLGA nanospheres optimized by design of experiments for ocular administration of dexibuprofen– in vitro, ex vivo and in vivo characterization. *Colloids and Surfaces B: Biointerfaces* **145,** 241–250 (2016).

52. Radhakrishnan, R., Kulhari, H., Pooja, D., Gudem, S., Bhargava, S., Shukla, R. *et al.* Encapsulation of biophenolic phytochemical EGCG within lipid nanoparticles enhances its

stability and cytotoxicity against cancer. *Chemistry and Physics of Lipids* **198,** 51–60 (2016).

53. Frank, A. Factors affecting the degradation and drug-release mechanism ofpoly(lactic acid) and poly[(lactic acid)-co-(glycolic acid)]. *Polym. Int* **54,** 36–46 (2005).

54. Singh R, Kesharwani P, Mehra NK, Singh S & Banerjee S, J. N. Development and characterization of folate anchored Saquinavir entrapped PLGA nanoparticles for anti-tumor activity. *Drug Dev. Ind. Pharm* **4,** 1888–1901 (2015).

55. Yao, F. & Weiyuan, J. K. Drug Release Kinetics and Transport Mechanisms of Non- degradable and Degradable Polymeric Delivery Systems. *Expert Opinion Drug Delivery* **7,** 429–444 (2010).

56. Li, S. & Huang, L. Pharmacokinetics and Biodistribution of Nanoparticles. *Molecular Pharmaceutics* **5,** 496–504 (2008).

57. Bankstahl, J. P. & Löscher, W. Resistance to antiepileptic drugs and expression of P-glycoprotein in two rat models of status epilepticus. *Epilepsy Research* **82,** 70–85 (2008).

58. Klee, R., Brandt, C., Töllner, K. & Löscher, W. Various modifications of the intrahippocampal kainate model of mesial temporal lobe epilepsy in rats fail to resolve the marked rat-to-mouse differences in type and frequency of spontaneous seizures in this model. *Epilepsy & Behavior* **68,** 129–140 (2017).

59. Wohlfart, S., Gelperina, S. & Kreuter, J. Transport of drugs across the blood – brain barrier by nanoparticles. *Journal of Controlled Release* **161,** 264–273 (2012).

60. Hanisch, U.K. & Kettenmann, H. Microglia: active sensor and versatile effector cells in the normal and pathologic brain. *Nat. Neurosci.* **10,** 1387–1394 (2007).

Figure legends

Figure 1. Optimization of EGCG NPs. **(A)** Z_{av} surface response at a fix EGCG concentration of 1.5 mg/ml, **(B)** PI response at a fix PLGA-PEG concentration of 14 mg/ml, **(C)** ZP Pareto's diagram. (**D**) TEM image of EGCG loaded PLGA-PEG NPs. Scale bar 2 μm/200 nm.

Figure 2. Interaction studies of EGCG PEGylated-PLGA NPs compounds. **(A)** DSC thermograms **(B)** FTIR spectra.

Figure 3. (A) *In vitro* release profile of EGCG loaded PLGA-PEG NPs against free EGCG. **(B)** EGCG NPs backscattering profile at storage temperature 4°C and (**C)** storage temperature 25°C.

Figure 4. **(A)** Dose- and time-dependent effects of the NPs in hemolysis test. **(B)** *In vitro* study of cell viability in bEnd.3, astrocytes and PC12 cell lines.

Figure 5. EGCG plasma profiles following a single i.p. dose of free EGCG and EGCG NPs 30 mg/kg to mice.

Figure 6. Behavioural assessment score.

Figure 7. FJ^+ cells counts in different brain areas of WT+KA group. Staining images of dead neurons show KA toxicity distribution in all areas. Scale bar 60 μm.

Figure 8. Results of immunohistochemistry assays. (**A**) Iba1 and GFAP counts of positive cells (**B**) Iba1 immunohistochemistry and Hoetsch. (**C**) Reactive GFAP cells and Hoetsch. Scale bar 30μm/60μm.

Table 1. Values of the 2^3 + star central composite rotatable factorial design, parameters and measured responses.

	C.EGCG		C.PLGA-PEG		C.Tween®80		Z_{av} (nm)	PI	ZP (mV)	EE (%)
	Coded level	(mg/ml)	Coded level	(mg/ml)	Coded level	(%)				
Factorial points										
F1	-1	0.5	-1	12	-1	1.5	182.1 ± 1.9	0.152 ± 0.003	-25.9 ± 0.92	96.4 ± 1.4
F2	1	1.5	-1	12	-1	1.5	162.9 ± 3.0	0.140 ± 0.028	-24.7 ± 1.0	95.2 ± 0.7
F3	-1	0.5	1	16	-1	1.5	186.8 ± 0.2	0.098 ± 0.003	-24.1 ± 1.4	96.3 ± 1.3
F4	1	1.5	1	16	-1	1.5	187.1 ± 1.7	0.096 ± 0.004	-26.1 ± 0.5	95.8 ± 0.1
F5	-1	0.5	-1	12	1	2.5	181.7 ± 3.9	0.066 ± 0.007	-23.6 ± 0.9	95.9 ± 0.4
F6	1	1.5	-1	12	1	2.5	141.0 ± 6.8	0.063 ± 0.059	-22.7 ± 0.8	94.4 ± 1.8
F7	-1	0.5	1	16	1	2.5	176.6 ± 1.5	0.053 ± 0.032	-23.3 ± 0.5	96.4 ± 0.3
F8	1	1.5	1	16	1	2.5	167.2 ± 3.5	0.081 ± 0.022	-24.1 ± 0.0	95.3 ± 2.3
Axial points										
F9	-1.68	0.16	0	14	0	2	187.1 ± 9.1	0.096 ± 0.131	-27.1 ± 2.8	96.2 ± 0.4
F10	1.68	1.85	0	14	0	2	158.9 ± 3.4	0.151 ± 0.021	-27.1 ± 2.0	95.6 ± 0.4
F11	0	1	-1.68	10.6	0	2	152.5 ± 0.2	0.059 ± 0.003	-23.6 ± 0.7	95.8 ± 1.8
F12	0	1	1.68	17.4	0	2	183.2 ± 9.2	0.087 ± 0.019	-25.3 ± 2.4	96.3 ± 2.1
F13	0	1	0	14	-1.68	1.16	192.9 ± 3.4	0.111 ± 0.051	-27.9 ± 0.4	96.0 ± 2.6
F14	0	1	0	14	1.68	2.84	154.0 ± 0.5	0.044 ± 0.053	-22.6 ± 1.1	97.3 ± 1.9
Central points										
F15	0	1	0	14	0	2	172.7 ± 2.3	0.151 ± 0.054	-26.9 ± 0.1	97.3 ± 0.3
F16	0	1	0	14	0	2	169.4 ± 2.3	0.125 ± 0.054	-27.1 ± 0.1	96.9 ± 0.2

Table 2. Results obtained in the behavioral seizure assessment. Experiment duration 2h (24 periods of 5 minutes)

		Groups		
		WT+KA n=10	**WT+KA+ free EGCG** n=16	**WT+KA+ EGCG NPs** n=16
Seizure Behaviours	**Scale rate**	**Number of periods**		
Normal behaviour	0	0.50±0.00	4.94±3.35	8.94±2.74
Immobility	1	7.50±4.69	14.00±3.99	13.00±3.99
Rigidity	2	8.10±4.86	3.12±3.07	0.87±0.71
Automatisms	3	2.20±1.42	1.00±1.75	0.81±1.07
Clonus and falling	4	1.30±1.60	0.75±0.89	0.37±1.00
Repetitions of falls	5	1.10±1.71	0.06±0.00	0
Severe seizures	6	1.10±1.71	0.06±0.00	0
Number of deaths		2	1	0
Seizure Score		41.00±6.57	26.03±7.77	18.70±5.21

Table 3. Pharmacokinetic parameters of i.p. administration of free EGCG and EGCG NPs 30 mg/kg in C57BL/6 mice.

Parameter	Unit	Free EGCG	EGCG NPs	P value
AUC[a]	ng/ml·min	87073.3±3775.0	7747.0±62080.0	0.0857
C_{max}	ng/ml	1375.8±324.8	565.1±90.5	0.0141
T_{max}	min	30.0±0.0	50.0±34.6	0.3739

Statistic was done with non-parametric t test for a non-compartmental i.p. input model. [a]AUC was measured between 0 to 240 minutes.

Graphical abstract

In this study Epigallocatechin-3-gallate loaded PEGylated-PLGA nanoparticles were developed for the treatment of temporal lobe epilepsy. The polymeric nanosystem protected the drug from degradation and improved the release of the drug into the brain. The results showed a significant reduction in the neurological alterations produced during the status epilepticus, such as number and intensity of seizures, neurotoxicity and neuroinflammation.

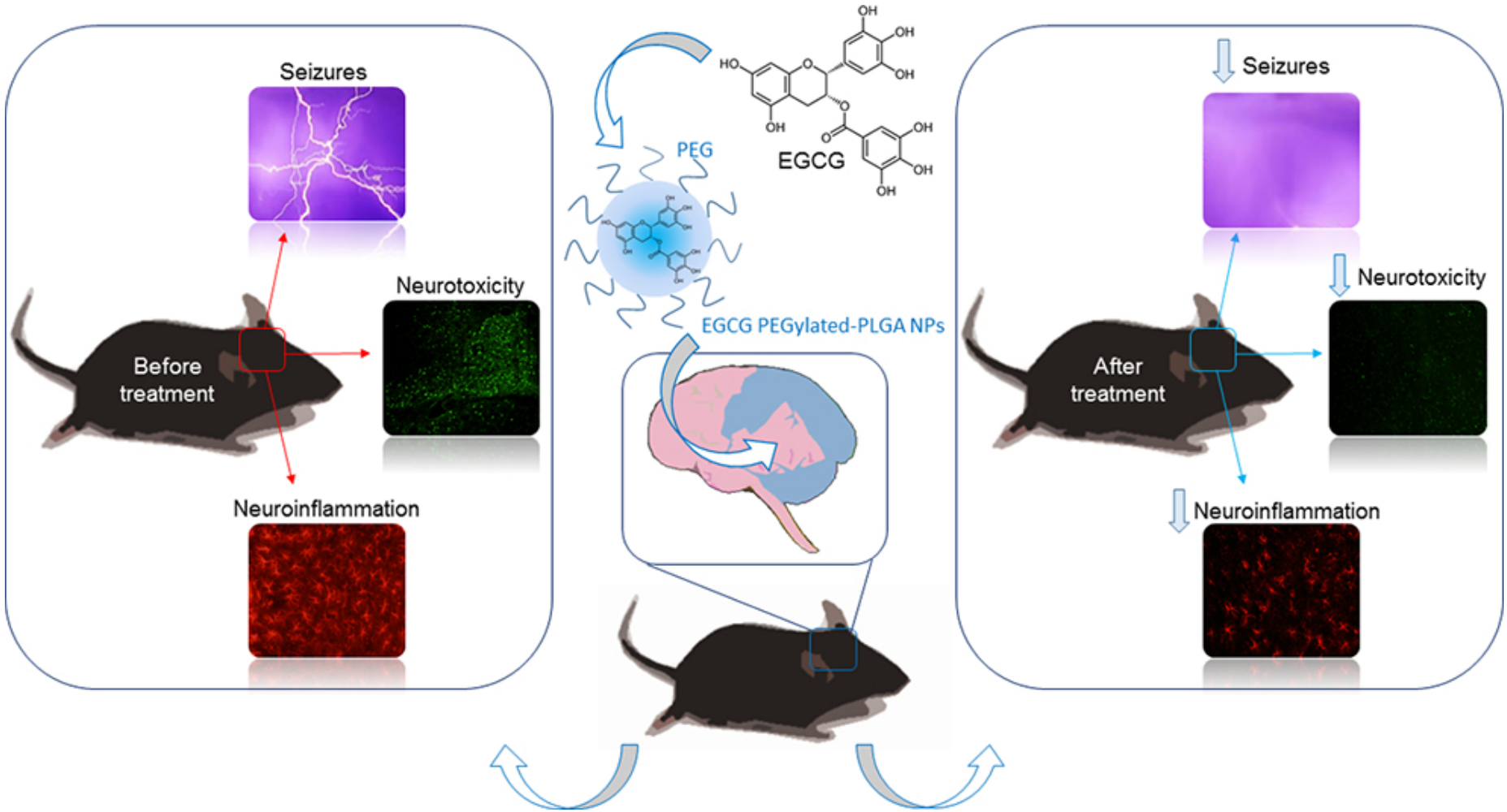

Graphics Abstract

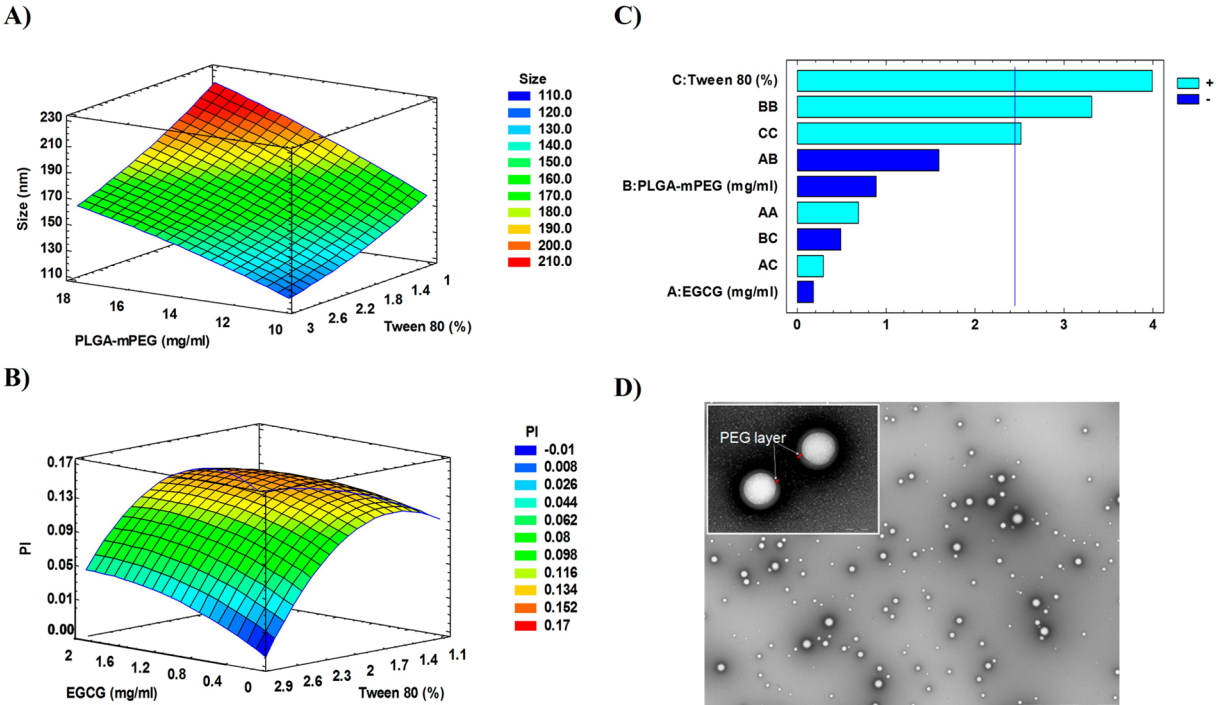
A)
Size (nm)
230
210
190
170
150
130
110
18
16
14
12
10
PLGA-mPEG (mg/ml)
3
2.6
2.2
1.8
1.4
1
Tween 80 (%)
Size
110.0
120.0
130.0
140.0
150.0
160.0
170.0
180.0
190.0
200.0
210.0
B)
PI
0.17
0.13
0.09
0.05
0.01
0.00
2
1.6
1.2
0.8
0.4
0
EGCG (mg/ml)
2.9
2.6
2.3
2
1.7
1.4
1.1
Tween 80 (%)
PI
-0.01
0.008
0.026
0.044
0.062
0.08
0.098
0.116
0.134
0.152
0.17
C)
C:Tween 80 (%)
BB
CC
AB
B:PLGA-mPEG (mg/ml)
AA
BC
AC
A:EGCG (mg/ml)
0
1
2
3
4
+
-
D)
PEG layer

Figure 1

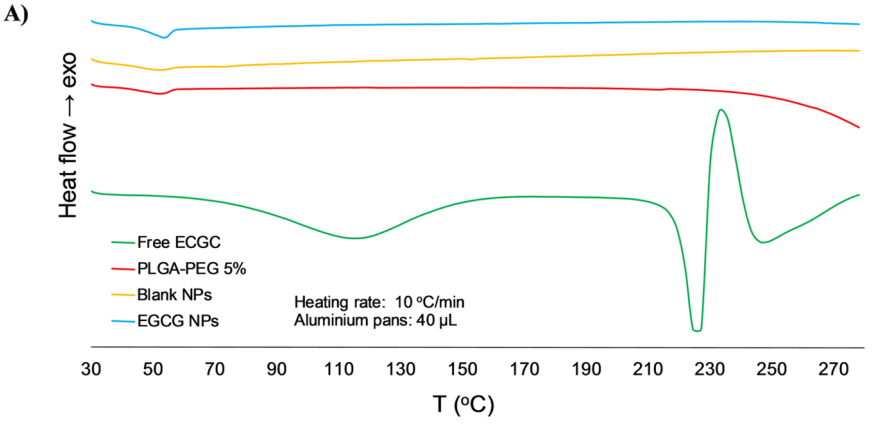
A)
Heat flow → exo
Free ECGC
PLGA-PEG 5%
Blank NPs
EGCG NPs
Heating rate: 10 °C/min
Aluminium pans: 40 µL
30 50 70 90 110 130 150 170 190 210 230 250 270
T (°C)

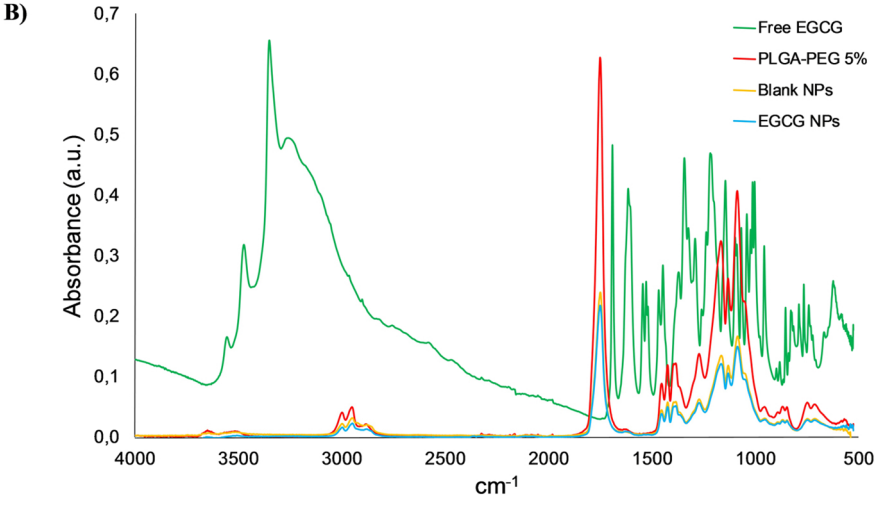
B)
Absorbance (a.u.)
0,7 0,6 0,5 0,4 0,3 0,2 0,1 0,0
Free EGCG
PLGA-PEG 5%
Blank NPs
EGCG NPs
4000 3500 3000 2500 2000 1500 1000 500
cm-1

Figure 2

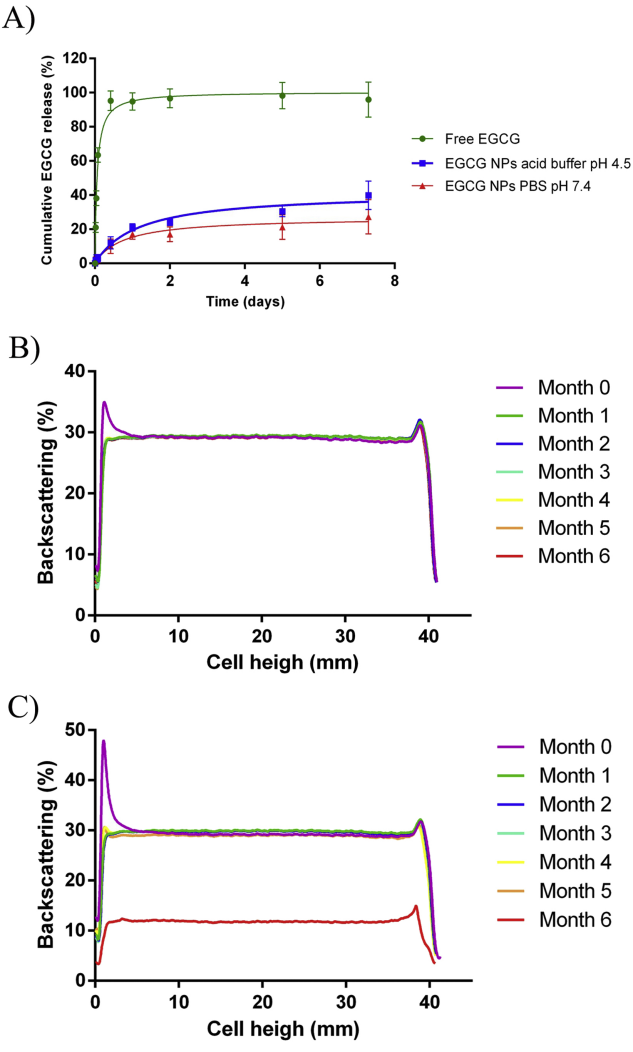
A)
Cumulative EGCG release (%)
120
100
80
60
40
20
0
0
2
4
6
8
Time (days)
Free EGCG
EGCG NPs acid buffer pH 4.5
EGCG NPs PBS pH 7.4
B)
Backscattering (%)
40
30
20
10
0
0
10
20
30
40
Cell heigh (mm)
Month 0
Month 1
Month 2
Month 3
Month 4
Month 5
Month 6
C)
Backscattering (%)
50
40
30
20
10
0
0
10
20
30
40
Cell heigh (mm)
Month 0
Month 1
Month 2
Month 3
Month 4
Month 5
Month 6

Figure 3

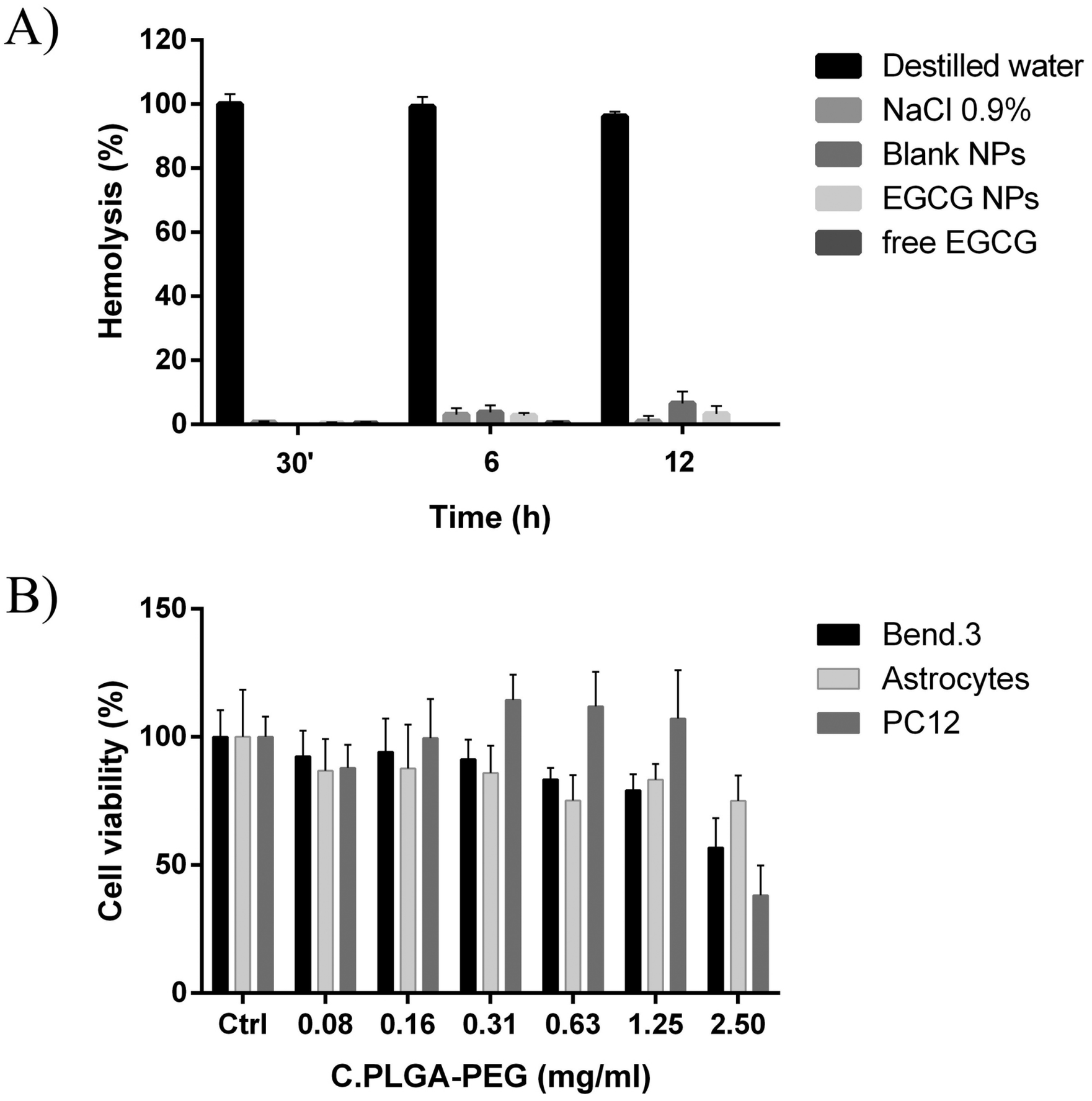
A)
120
100
80
60
40
20
0
Hemolysis (%)
30'
6
12
Time (h)
Destilled water
NaCl 0.9%
Blank NPs
EGCG NPs
free EGCG
B)
150
100
50
0
Cell viability (%)
Ctrl
0.08
0.16
0.31
0.63
1.25
2.50
C.PLGA-PEG (mg/ml)
Bend.3
Astrocytes
PC12

Figure 4

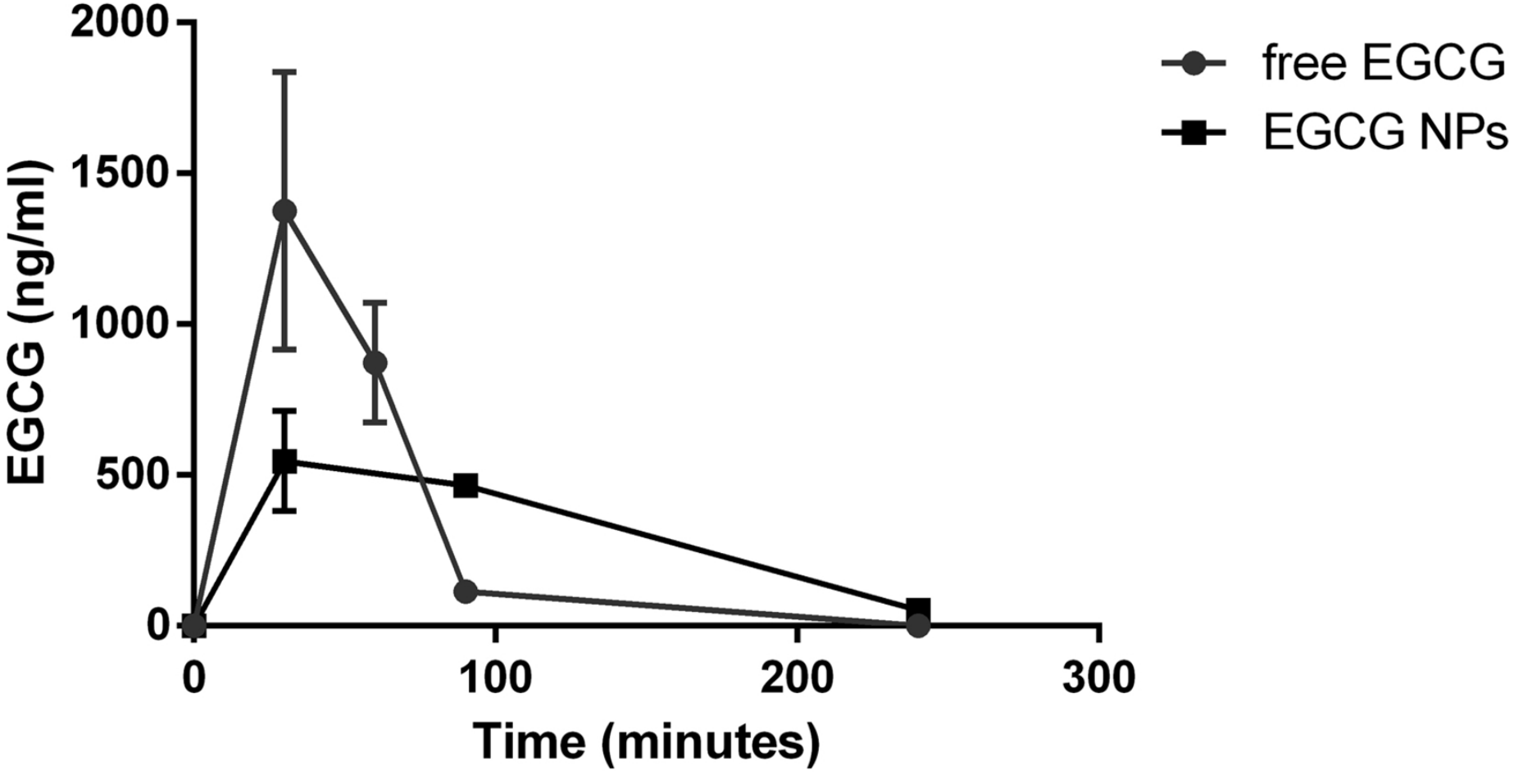
2000
1500
1000
500
0
EGCG (ng/ml)
0
100
200
300
Time (minutes)
free EGCG
EGCG NPs

Figure 5

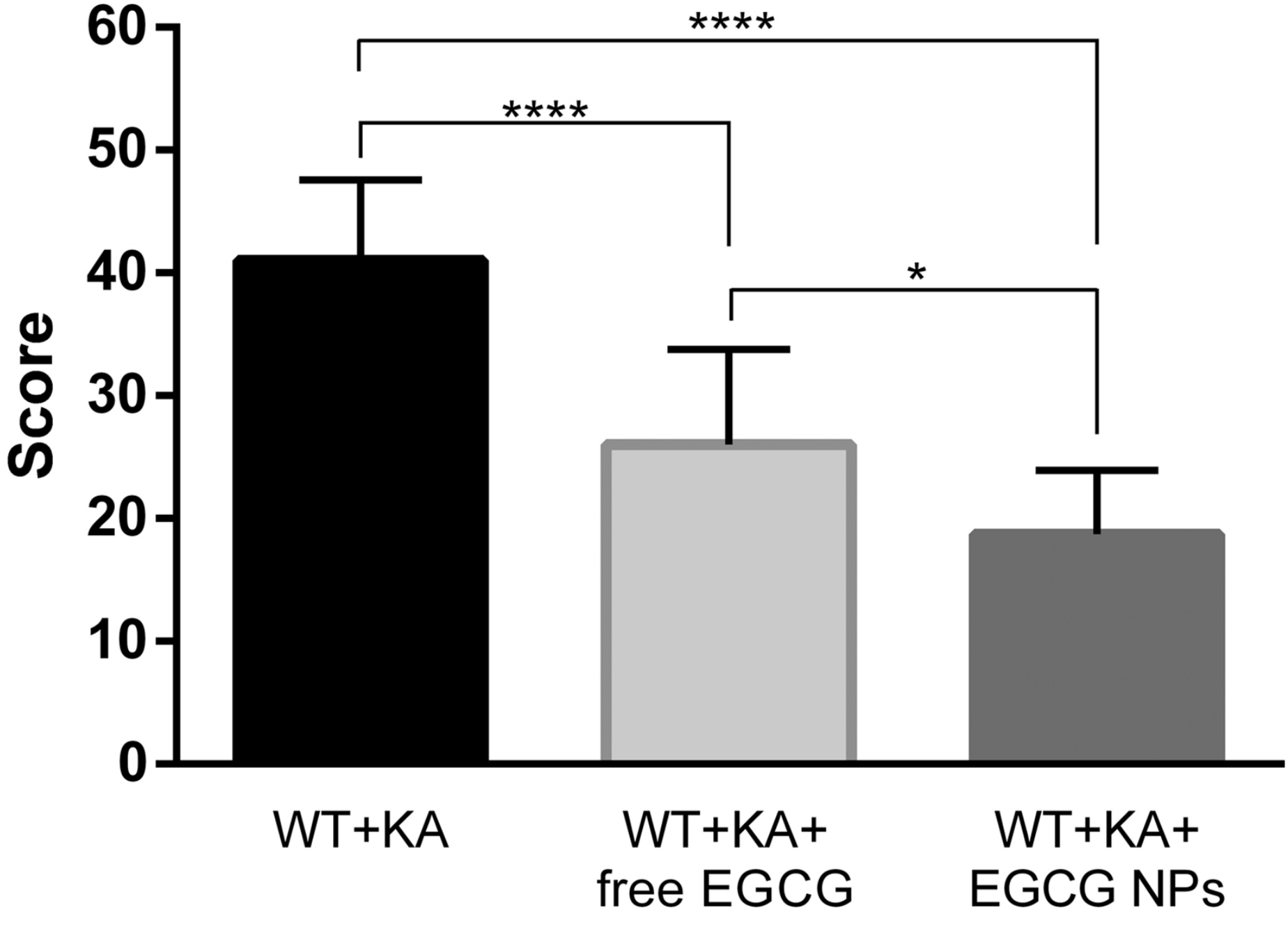

Figure 6

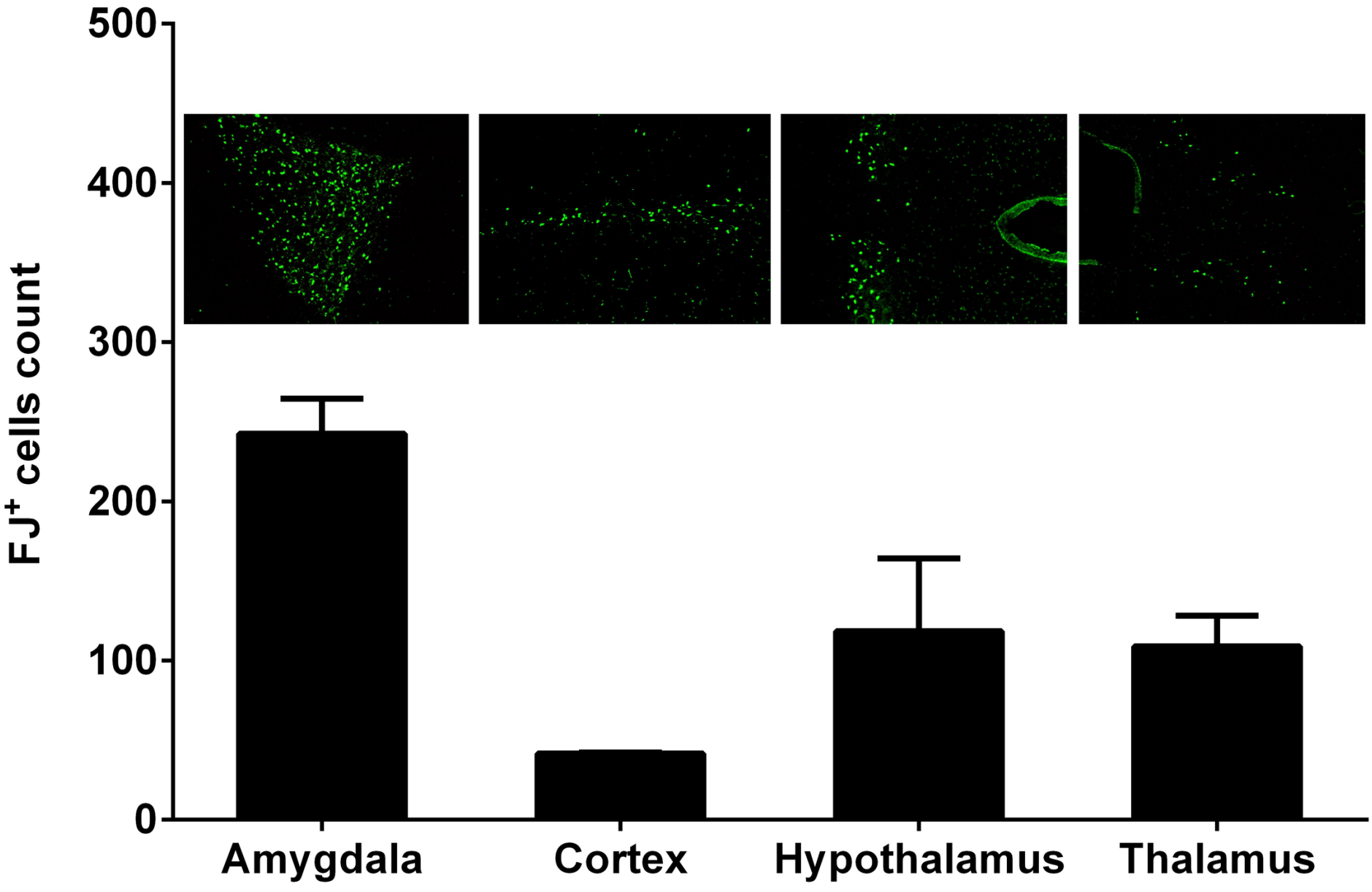
500
400
300
200
100
0
FJ+ cells count
Amygdala
Cortex
Hypothalamus
Thalamus

Figure 7

A)

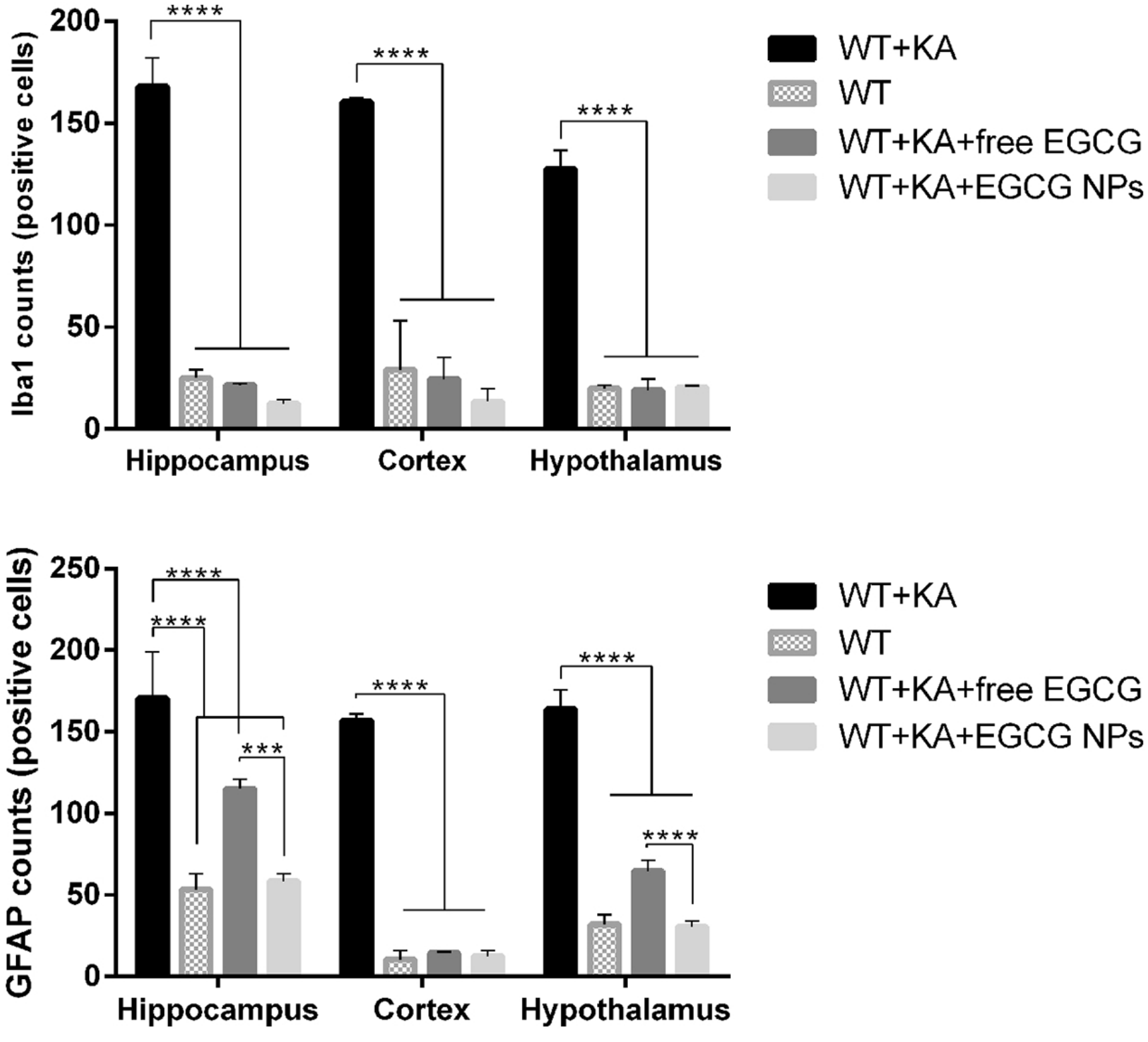
Iba1 counts (positive cells)
200
150
100
50
0
****
****
****
Hippocampus
Cortex
Hypothalamus
WT+KA
WT
WT+KA+free EGCG
WT+KA+EGCG NPs
GFAP counts (positive cells)
250
200
150
100
50
0
****
****
***
****
****
****
Hippocampus
Cortex
Hypothalamus
WT+KA
WT
WT+KA+free EGCG
WT+KA+EGCG NPs

Figure 8a

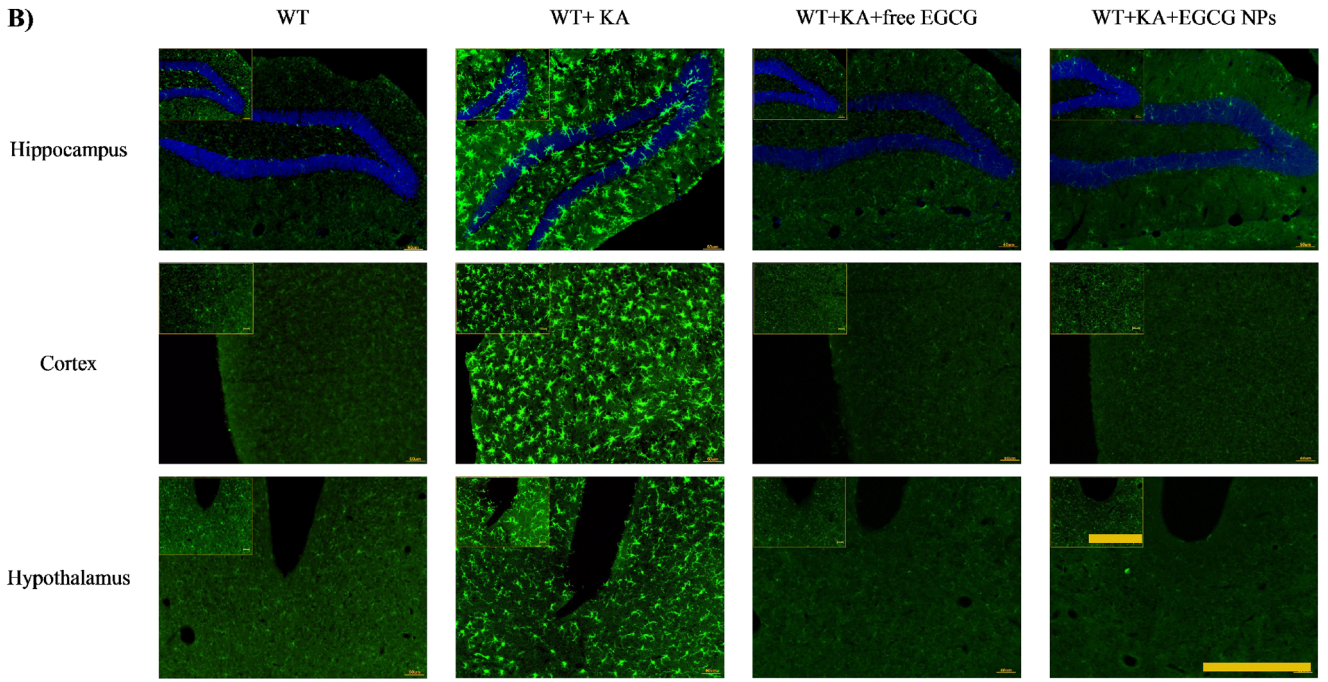
B)
WT
WT+ KA
WT+KA+free EGCG
WT+KA+EGCG NPs
Hippocampus
Cortex
Hypothalamus

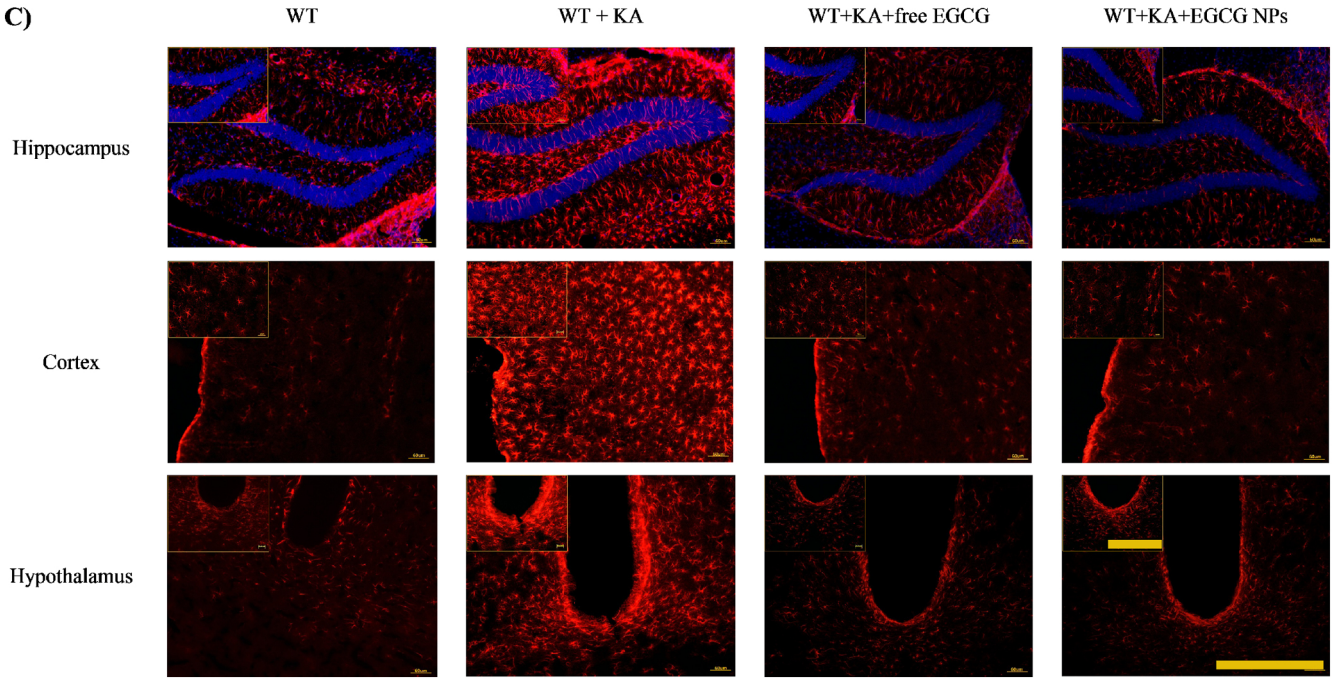
C)
WT
WT + KA
WT+KA+free EGCG
WT+KA+EGCG NPs
Hippocampus
Cortex
Hypothalamus

Figure 8bc